

## Supplementary information

### Crossing Interfacial Conduction in Nanometer-Sized Graphitic Carbon Layers

Manabu Tezura and Tokushi Kizuka\*

*Department of Material Science, Faculty of Pure and Applied Sciences, University of Tsukuba,  
1-1-1, Tennoudai, Tsukuba, Ibaraki 305-8573, Japan*

\* Corresponding author

Supplementary Information contains the captions of Movies 1 and 2, and Sections 1–4.

#### Movie captions

**Movie 1:** Movie of the structural dynamics of the contact interface between the CNC and the negative Au electrode using the piezomanipulation system corresponding to Figures 1(b-1) and 1(b-2). Three halfway time-ranges are skipped and their elapsed times are presented.

**Movie 2:** Movie of the contact process between the CNC and the Au electrodes corresponding to Figs. S2(a)–(d). Note that the structure of the contact interface in the negative electrode side changes, whereas that in the positive electrode side was fixed.

#### Sections 1–4

##### Section 1: Current–voltage characteristic of the SNPJ presented in Figure 1(a).

The current of the SNPJ in Figure 1(a) was measured after the structures of the contact interfaces between the CNC and two Au electrodes were fixed. The slope (total resistance) near 13 mV, which was the bias voltage for the resistance measurement, was estimated to be 4.7 k $\Omega$ .

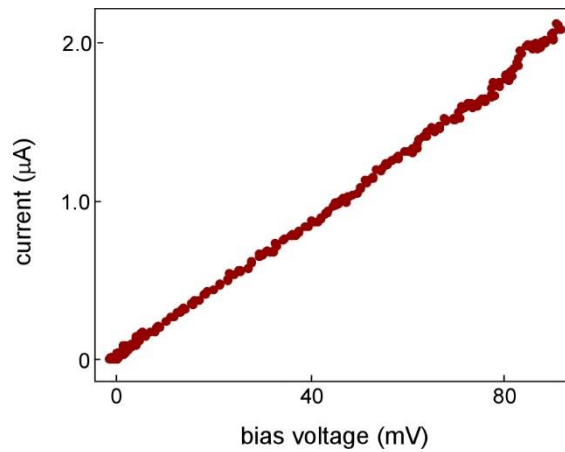


**Figure S1.**

**Section 2: The dependency of the total resistance of a SNPJ on the negative-side contact area.**

Figures S2 and S3 show the high-resolution TEM images of a compressing process between a CNC and Au electrodes and the variations in the total resistance of the SNPJ, respectively. Times a–d are the observation times of Figs. S2(a)–(d), respectively. The contact area between the CNC and the negative Au electrode was increased due to compressing by the displacement of the Au electrode, resulting in the decrease in the total resistance. The contact area at times a–d was 13.0, 17.4, 19.1, and 24.7 nm<sup>2</sup> and the corresponding total resistance was 8.2, 7.3, 6.5, and 4.7 kΩ, respectively. In this process, the larger contact area of 90.2 nm<sup>2</sup> between the CNC and the positive Au electrode was not changed. Thus, the resistance of the SNPJ depended on only the negative-side contact area. For the influence of the pressure on the significant decrease in the resistance, see Discussion in the main text.

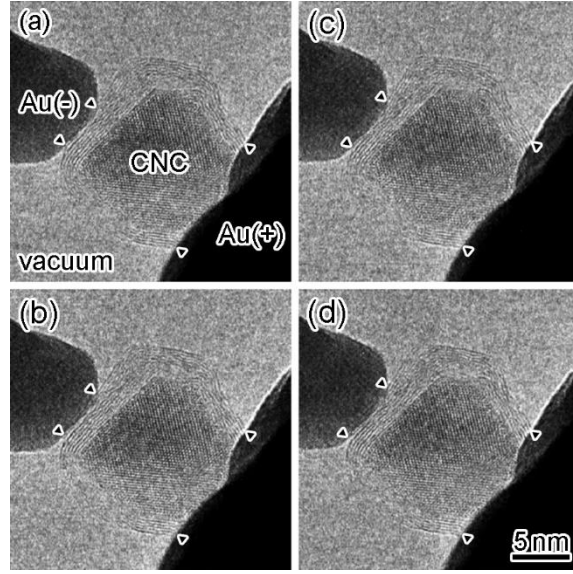


Figure S2.

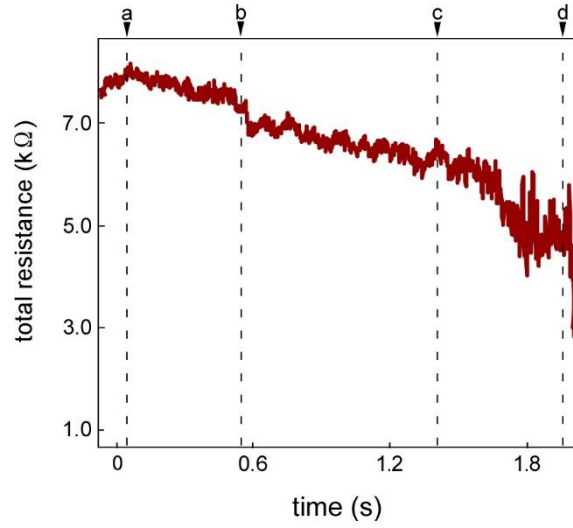


Figure S3.

### Section 3: Calculation of $G^u$ of nanometer-sized GCL/Au interfaces.

Transmission probability of  $i$ -th C atom (the  $C_i$  atom) ( $T_i$ ) at a GCL/Au interface is the sum of the transmission probabilities between the  $C_i$  atom and the neighboring  $n_{Au}$ -number of Au atoms at the interface.  $T_i$  is given by the equation <sup>1</sup>:

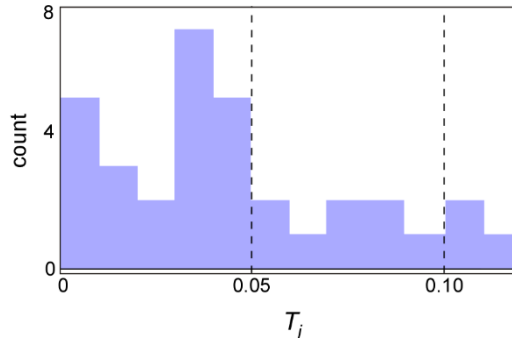
$$T_i = \sum_j^{n_{Au}} T_{ij} \quad (S1).$$

Figure S4 shows the histogram of  $T_i$  obtained by the first-principle calculation for the model of the GCL/Au interface shown in Figure 3(a). The average value of  $T_i$  ( $\bar{T}_i$ ) was 0.0431.

The Landauer formula is defined as:  $G = (2e^2/h)\sum T_{ij}$ , where  $2e^2/h (=G_0)$  is the quantum unit,  $e$  is the electron charge, and  $h$  is Planck's constant.<sup>1</sup> Hence,  $G^u$  is expressed as:

$$G^u = G/n_C = (G_0 \sum T_i)/n_C = G_0 \bar{T}_i, \quad (\text{S2})$$

where  $n_C$  is the total number of the C atoms in the GCL/Au interfaces.  $\bar{T}_i$  was estimated from the first-principles calculation, and by substituting it for  $\bar{T}_i$  in Equation S2,  $G^u$  was estimated.



**Figure S4 Histogram of  $T_i$  on a GCL/Au interface.**

#### **Section 4: The first-principle calculation for a LaC<sub>2</sub>/GCL/Au interface**

An encapsulating LaC<sub>2</sub> crystal in a CNC was located at the center of the eight spherical C shell-layers, and a LaC<sub>2</sub>/GCL interface was formed. We investigated the influence of the LaC<sub>2</sub> crystals on the electronic states of the C layers. The models of the atomic configurations of the LaC<sub>2</sub>/GCL/Au interfaces were constructed on the basis of the observed high-resolution TEM images, and the first-principle calculation was performed to investigate the density of states (DOS) of the entire systems of the interfaces and the partial density of states (PDOS) of the C layers adjacent to the Au electrode. On the basis of the observed TEM images,  $d_i$  and the orientational relationship of the LaC<sub>2</sub>/GCL/Au interfaces were selected to the same manner as

those for the models shown in Figure 3. When the area and the number of the GCLs was selected to be  $\sim 1.4 \text{ nm}^2$  and two layers, respectively, the difference in the electronic states between  $\text{LaC}_2/\text{GCL}/\text{Au}$  and  $\text{GCL}/\text{Au}$  interfaces emerged. Figure S5(a) and S5(b) show the models of the atomic configurations of  $\text{LaC}_2/\text{GCL}/\text{Au}$  and  $\text{GCL}/\text{Au}$  interfaces. The results of the calculation of the DOS and the PDOS are shown in Figures S5(c) and S5(d), respectively. The DOS of the  $\text{LaC}_2/\text{C}/\text{Au}$  interface was different from that of the  $\text{LaC}_2$ -absent  $\text{C}/\text{Au}$  interface, reflecting their structural difference (Fig. S5(c)). In contrast, there was no effective difference in the PDOS near the Fermi energy of the C layer adjacent to the Au electrode. (Fig. S5(d) and the inserted diagram). These results show that the  $\text{LaC}_2$  crystal unlikely contribute to the PDOS of the C layers, which is associated with the conduction. In the SNPJs constructed of the eight spherical C shell-layers and the encapsulating  $\text{LaC}_2$  crystals at the center, and the  $\text{LaC}_2/\text{GCL}$  interfaces were located at the inner C shell-layers. From the above calculation results, the PDOS near the Fermi energy of the outermost C layer of the CNCs is not further influenced by the  $\text{LaC}_2$  crystals. Also considering the ratio of the c-axis resistivity to the in-plane resistivity ( $\sim 10^3$ ), it is considered that the most of conduction electrons pass through only the outermost C layer of the CNCs.

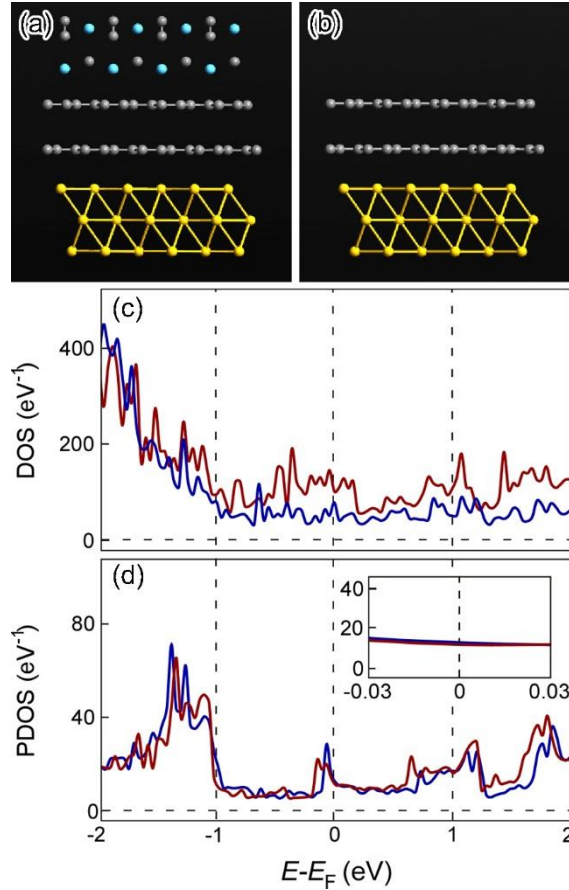


**Figure S5 DOS of the entire systems and PDOS of the C layer adjacent to the Au electrode for the LaC<sub>2</sub>/GCL/Au and the GCL/Au interfaces.** (a, b) The models of the atomic configurations used for calculation; (a) LaC<sub>2</sub>/GCL/Au interface and (b) GCL/Au interface. Both the models are projected along the direction parallel to the interfaces. The smaller gray circles, the larger yellow circles, and the larger light blue circles represent the the atomic columns of C, Au, and La atoms, respectively. (c) DOS of the entire systems of the both interfaces. The red and blue lines represent the results for the LaC<sub>2</sub>/GCL/Au and the GCL/Au interfaces, respectively. (d) PDOS of the C layer adjacent to the Au electrode for both interfaces. The enlarged PDOS near the Fermi energy is inserted. As for the color of each line, refer to (c).

## Reference

- 1 S. Datta, *Electronic Transport in Mesoscopic Systems*, Cambridge Univ. Press, Cambridge, 2013.